Article

Not peer-reviewed version

Vertical Variations of Leaf Photosynthetic and Biochemical Parameters Within Winter Wheat and Paddy Rice Canopies at Different Growth Stages

Jing Li , Yanlian Zhou , Xuehe Lu , Tingting Zhu , Kai Cao , Shucun Sun , Bo Tang * , Weimin Ju *

Posted Date: 13 April 2026

doi: 10.20944/preprints202604.0820.v1

Keywords: maximum carboxylation rate at 25 °C (Vc_{max25}); maximum electron transport rate at 25 °C (J_{max25}); leaf nitrogen content; leaf chlorophyll content; winter wheat; paddy rice

 doi:10.20944/preprints202604.0820.v1

Article

Vertical Variations of Leaf Photosynthetic and Biochemical Parameters Within Winter Wheat and Paddy Rice Canopies at Different Growth Stages

Jing Li [1,2,3], Yanlian Zhou [2], Xuehe Lu [4], Tingting Zhu [5], Kai Cao [1], Shucun Sun [3], Bo Tang [1,6,*] and Weimin Ju [2,*]

[1] Ecological and Environmental Science and Research Institute of Zhejiang Province, Hangzhou, 310007, China
[2] International Institute for Earth System Sciences, Nanjing University, Nanjing, 210023, China
[3] School of Life Sciences, Nanjing University, Nanjing 210023, China
[4] School of Geography Science and Geomatics Engineering, Suzhou University of Science and Technology, Suzhou, 215000, China
[5] State Key Laboratory of Soil and Sustainable Agriculture, Institute of Soil Science, Chinese Academy of Sciences, Nanjing 211135, China
[6] Zhejiang Key Laboratory of Ecological Environmental Damage Control and Value Transformation, Hangzhou, 310007, China
* Correspondence: tangbo1984278@163.com (B.T.); juweimin@nju.edu.cn (W.J.); Tel.: +86 0571-87998939 (B.T.)

Abstract

During crop growth, leaf photosynthetic capacity changes continuously, and the vertical distribution of leaf nitrogen (N_a) and chlorophyll (Chl_a) affects photosynthesis in different canopy layers. Understanding stratified photosynthesis is vital for accurate prediction of crop photosynthetic capacity. We conducted a two-year field study on winter wheat and paddy rice in Eastern China, measuring leaf maximum carboxylation rate (V_{cmax25}), maximum electron transport rate (J_{max25}), N_a, and Chl_a every 7–10 days from greening to maturity. We analyzed vertical variations of these parameters in upper (T-1), middle (T-2), and lower (T-3) canopy layers and explored relationships between N_a/Chl_a and V_{cmax25}. Results showed significant vertical variations: V_{cmax25} and J_{max25} in T-1 were higher than T-2, and T-2 higher than T-3. The vertical distribution of N_a and V_{cmax25} was more pronounced than Chl_a. Correlation between N_a and V_{cmax25} increased from T-1 to lower layers, while V_{cmax25}-Chl_a correlation decreased. A single V_{cmax25} estimation model based on N_a performed well across layers (R^2=0.619, RMSE=15.751 μmol m^{-2} s^{-1}). Differentiating T-1 from T-2/T-3 improved Chl_a-based models. N_a was better than Chl_a for characterizing V_{cmax25} vertical variation, with Chl_a-based models requiring separation of T-1 from T-2/T-3. This study provides key insights for remote sensing of photosynthetic parameters and improves understanding of crop canopy photosynthesis.

Keywords: maximum carboxylation rate at 25 °C (V_{cmax25}); maximum electron transport rate at 25 °C (J_{max25}); leaf nitrogen content; leaf chlorophyll content; winter wheat; paddy rice

1. Introduction

Photosynthesis is one of the most important chemical reactions on the earth, and about 90% of the dry matter accumulated by plants comes from photosynthetic products [1,2]. The photosynthetic capacity of plant leaves exhibits considerable variability within canopies, which leads to spatial heterogeneity in overall canopy photosynthesis [3–8]. As the structure of the vegetation canopy changes, leaves can acclimate to varying light conditions by adjusting components involved in photosynthetic mechanisms within a few days [3]. For example, leaf nitrogen (N), which is highly mobile within plants, can be redistributed effectively to rapidly optimize whole-plant photosynthesis

 doi:10.20944/preprints202604.0820.v1

[7,9]. Studies have demonstrated that the vertical distribution of N within the canopy is closely associated with light gradients, generally following the Beer-Lambert law [10]. Specifically, the cumulative leaf area index (LAI) decreases exponentially from the top of the canopy downward as the cumulative LAI increases [11]. The attenuation of light in the canopy led to the vertical variations of leaf morphology and physiological parameters. The leaves in the upper layer had more activated Rubisco enzyme, its net photosynthetic rate (A_n) is often higher than that of leaves in the lower layers [12,13].

In most terrestrial biosphere models (TBMs), the net photosynthetic rate (A_n) of vegetation leaves is calculated using the Farquhar-von Caemmerer-Berry (FvCB) model [14], and A_n is controlled by carboxylase reaction rate and electron transfer rate. The maximum carboxylation rate at 25℃ (V_{cmax25}) and maximum electron transfer rate at 25℃ (J_{max25}) are two key parameters of the FvCB model. V_{cmax25} is a kinetic parameter that characterizes ribulose 1,5-diphosphate carboxylase (Rubisco) in the Calvin cycle, and J_{max25} characterizes the effectiveness of cytochrome in transporting electrons to produce chemical energy transfer. On average, it takes two electrons to reduce one unit of Rubisco, which means that the ratio between J_{max25} and V_{cmax25} is generally constant. In TBMs, J_{max25} is usually determined by a linear empirical formula based on V_{cmax25} [15,16]. Thus, accurate estimates of V_{cmax25} are very important to simulate A_n and gross primary productivity (GPP) as errors in these two entities may be exacerbated when upscaling from leaf to ecosystem level [17].

V_{cmax25} has significant spatiotemporal variation characteristics [18,19]. Leaf V_{cmax25} is closely related to leaf nitrogen (N) and chlorophyll (Chl) contents [20,21]. Studies have shown that leaf nitrogen (normanlly expressed on an area basis in g m^{-2}, N_a) and Chl (normanlly expressed on an area basis in μg cm^{-2}, Chl_a) can be used as proxies of V_{cmax25}, yet the relative performance of the two proxies continues to be debated [22–24]. These studies focused only on the top leaves within plant canopies with sufficient light, neglecting the leaves in the middle and lower canopy layers. Quantitative studies specifically addressing the relationships between V_{cmax25} and N_a (Chl_a) in the middle and lower canopy layers of crops remain relatively scarce.

There were studies found that the vertical distribution of leaf N in the canopy affected the photosynthetic process of leaves at different positions in the canopy [8,25,26]. Leaves located in the upper layer of the vegetation canopy had more activated Rubisco enzyme, and V_{cmax25} and J_{max25} were higher than those in the lower layers. Therefore, TBMs estimate the average V_{cmax25} for plant canopy based on the assumption that the vertical variation pattern of V_{cmax25} inside the canopy aligns with that of nitrogen (N) content [23,27,28]. The estimation assumes that the vertical profile of V_{cmax25} in the middle and lower canopy layers mirrors exactly that of N. Moreover, studies exploring the relationship between V_{cmax25} and Chl have generally adopted the same assumption—often extrapolating V_{cmax25} values derived from upper-canopy leaves to estimate those in the middle and lower layers. However, there is insufficient empirical evidence to confirm that..

In the process of crop growth, vertical heterogeneity appears in wheat and rice canopies [29]. After entering the jointing stage, differences in light energy absorption capacity among leaf layers become more pronounced due to variations in leaf age and position, leading to significant differentiation in the photosynthetic capacity of leaves at different canopy levels. Therefore, without considering the differences in the non-uniform vertical distribution of leaf biochemical parameters, the accuracy of monitoring the photosynthetic capacity and nutrient accumulation capacity of crops will be significantly affected, and the accuracy of estimated photosynthesis will be reduced. Previous studies have developed separate V_{cmax25}–Chl regression models for the pre-anthesis and post-anthesis periods and has found significantly reducded uncertainty in model simulations [21]. During the growing season of crops, the uptake, translocation, and redistribution of nitrogen in leaves undergo dynamic changes. Senescence advances from the basal leaves upward, while the flag leaves remain green, forming distinct vertical heterogeneity of photosynthesis capacity within the canopy [30]. Therefore, it is essential to understand the characteristics of crop photosynthesis and physiology, and to obtain the photosynthetic capacity, biochemical parameters of the upper, middle and lower layers of crop canopy, so as to improve the prediction accuracy of photosynthetic capacity.

 doi:10.20944/preprints202604.0820.v1

In this study, we took a two-year field observation of winter wheat and paddy rice in eastern China. We measured V_{cmax25}, J_{max25}, N and Chl within canopies of winter wheat and paddy rice across multiple growth seasons. The objectives of the study are: (1) to study the seasonal and vertical patterns of photosynthetic parameters V_{cmax25}, J_{max25}, N and Chl of winter wheat and paddy rice leaves within canopies; (2) to investigate the relationships between V_{cmax25} and N (Chl) within canopies, and whether the characteristics of this relationship vary across growth stages.

2. Materials and Methods

2.1. Field Sites

Field campaigns were conducted at two farmlands in Jurong and Shangqiu, China (Figure 1). The first site is located at the Jurong Ecological Observation Station (JROS, 31.81°N, 119.22°E, and elevation 15 m above the sea level), Jurong city, Jiangsu Province, China. This station is characterized as northern subtropical monsoon climate, with an average annual temperature of 15.5°C and average annual precipitation of 1099.1 mm. Further information about this site was described by Dai and Li [31,32]. The second site is an experimental station of the Farmland Irrigation Research Institute, Chinese Academy of Agricultural Sciences, located in Shangqiu, Henan province, China (SQOS, 34.52°N, 115.59°E, elevation 52 m). The site is a typical wheat-growing region in China, located in a warm temperate continental monsoon climatic region, with annual precipitation of 708 mm, mean temperature of 13.9 °C, sunshine duration of 2398 h [33].

Measurements were conducted for winter wheat (*Triticum aestivum L.*, Aizhuang58) at SQOS (2018), and for paddy rice (*Oryza sativa L.*, Nanjing5508) at JROS (2017, 2018). Winter wheat was sown at late October in 2017 at SQOS and harvested at late May next year. At JROS, paddy rice seeds were sown in early May, and the seedlings were transplanted in middle June and harvested in late October. Further detail about crops cultivation was described by Li [32]. Our observations were conducted about every 7 to 10 days during the growing seasons of winter wheat and paddy rice (Figure 1). The top 3 leaves (labeled T-1, T-2, and T-3, respectively) of plants were measured for studies found that the top 3 leaves contributed more than 90% to the yield of winter wheat and paddy rice[34]. The observation period commenced with the winter wheat at the greening stage and the paddy rice at the tillering stage.

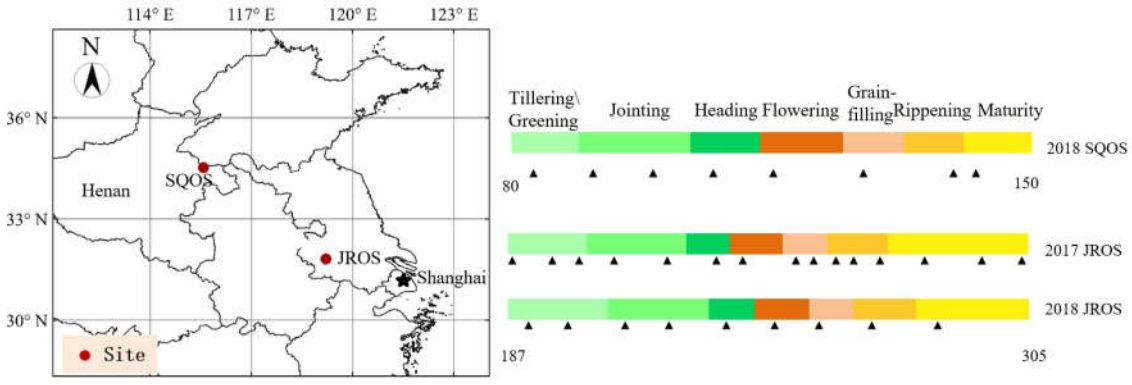

Figure 1. Locations of two sites with observations conducted (left) and the day of year (DOY) for different growth stages and observations at two sites (right). On the right panel, colors represent duration of different growth stages and black triangles indicate DOYs of observations. (Note: this image is a modified version, and a similar image have published in previous studies of the same series by our team [21]).

2.2. Measurements of Leaf Gas Exchange

At each sampling event, three independent, representative plants were selected as biological replicates, and the top three fully expanded leaves (T-1, T-2, T-3) were measured for gas exchange. Layer-specific values for each date were then calculated as the mean of the three biological replicates.

 doi:10.20944/preprints202604.0820.v1

This design yielded a total of 69 leaf photosynthetic parameters estimates for winter wheat (2018) and 192 for paddy rice (2017–2018), forming the basis for all subsequent statistical modeling.

In 2018 at SQOS, we measured leaf-level gas exchanges on expanded leaves of three labeled winter wheat plants using a portable photosynthesis system (LI-6800, LI-COR, Lincoln, NE, USA). The CO_2 response curves (A_n-C_i curves) were produced under conditions of saturated photosynthetic photon flux density (PPFD) (1800 μmol m−2 s−1) and stepwise CO_2 concentrations of 400, 200, 150, 100, 50, 400, 400, 600, 800, 1000, 1200, 1500 ppm. From March 25 (tillering stage) to May 23 (maturity stage), eight measurements were taken on each plant, obtaining 24 top leaf (T-1), 24 middle leaf (T-2), and 21 lower leaf (T-3) samples, yielding a total of 69 leaf-level observations (69 A_n-C_i curves in total).

At JROS, A_n-C_i curves were measured by LI-6400XT in 2017 and by LI-6800 in 2018. Both the LI-6400XT and LI-6800 instruments were routinely calibrated according to the manufacturer's protocols before each measurement campaign. For paddy rice, photosynthetic observations were conducted over 15 campaigns (7 July–30 October 2017) and 9 campaigns (10 July–11 October 2018), respectively. A total of 192 A_n-C_i curves were generated in 2017 (117 samples in total: 45 from T-1, 36 from T-2, 36 from T-3) and 75 curves in 2018 (75 samples in total: 27 from T-1, 24 from T-2, 24 from T-3).

Leaf gas exchange data were analyzed and A_n-C_i curves were fitted using the 'plantecophys' R package [35] to estimate photosynthetic parameters V_{cmax25} and J_{max25}. These parameters were then normalized to 25 °C using the Arrhenius temperature response function [36]. More detail was described by Li [21].

2.3. Measurements of Leaf Biochemical Parameters

We sampled leaves from 3 plants adjacent to those used for A_n-C_i curve measurements, targeting the same canopy positions (top, middle, lower layers) to ensure consistency. A SPAD-502 portable chlorophyll meter (Konica Minolta Inc., Osaka, Japan) was used to select leaves for chlorophyll (Chl) and nitrogen (N) analysis—only those with SPAD readings matching the A_n-C_i curve leaves (±2) were included. Subsequent laboratory analyzes quantified Chl and N content, with leaf N expressed as area-based units (g m^{-2}) and Chl as area-based units (μg cm^{-2}). Detailed protocols for Chl and N measurement were described by Li [21].

2.4. Analysis

The V_{cmax25}, J_{max25}, N_a and Chl_a from the three sampled leaves were averaged to represent the campaign-level values. The seasonal patterns of these parameters across canopy layers were examined. Then, linear regression models relating V_{cmax25} to N_a and Chl_a were developed separately for paddy rice and winter wheat. The experimental data were collected from two field sites—Jurong and Shangqiu —over multiple years: paddy rice in 2017 and 2018, and winter wheat in 2018. To evaluate whether a generalized V_{cmax25} estimation model could be developed across these varying environmental and temporal conditions, we first pooled all observations, we applied dummy variable regression analysis [37]. Dummy variable regression analysis is a widely used method to determine whether the coefficients of different regression lines are significantly different [21].

To investigate how species (paddy rice vs. winter wheat) and growth stages influence these relationships, We employed dummy variable regression analysis to test whether the intercepts and slopes of the linear estimation models relating V_{cmax25} to N_a or Chl_a in paddy rice differed significantly from those in winter wheat. Furthermore, we evaluated whether a unified linear model—based on N_a or Chl_a—could be applied across the entire growing season for both crops. Model performance was evaluated using the coefficient of determination (R^2), root mean square error (RMSE), and the p-values of regression coefficients. Due to the limited number of observational samples, the established linear estimation model of V_{cmax25} based on N_a and Chl_a was validated using the Leave-One-Out Cross-Validation (LOO-) method. All statistical analyses and model diagnostics were conducted in R (version 4.3.1) and Microsoft Excel 2019 (Microsoft, Redmond, WA, USA).

 doi:10.20944/preprints202604.0820.v1

3. Results

3.1. Seasonal Variations of Leaf N_a and Chl_a in Crop Canopies

N_a and Chl_a of T-1, T-2 and T-3 in the leaves of winter wheat (WW) and paddy rice (PR) exhibited distinct vertical and seasonal patterns (Figure 2). N_a of winter wheat leaves ranged from 0.81 to 2.31 $g{\cdot}m^{-2}$. The mean N_a values for T-1, T-2, and T-3 leaves were 1.89, 1.88, and 1.34 $g{\cdot}m^{-2}$, respectively, with standard deviations (SD) of 0.38, 0.37, and 0.34 $g{\cdot}m^{-2}$. Dynamically, the N_a of T-1 leaves initially decreased, then increased after the flag leaves were fully expanded, reaching a peak at the flowering stage. The N_a in T-2 leaves peaked at the jointing stage, slightly decreased during the heading to flowering stages, and then declined rapidly from the grain-filling to maturity stages. The variation trend of N_a in T-3 leaves was similar to that of T-2 . For paddy rice at JROS in 2017, the N_a ranged from 0.61 to 2.25 $g{\cdot}m^{-2}$, with mean values of 1.42, 1.19, and 1.09 $g{\cdot}m^{-2}$ for T-1, T-2, and T-3 leaves, respectively (Figure 2b). In 2018, the mean N_a of T-1, T-2 and T-3 were 1.66, 1.59 and 1.53 g m^{-2}, respectively. The seasonal trends of N_a across leaf layers in rice during both years were similar to those observed in winter wheat.

In 2018 at SQOS, Chl_a of winter wheat ranged from 24.28 to 82.47 μg cm^{-2}, and the mean Chl_a values of T-1, T-2 and T-3 leaves were 59.17, 57.39 and 47.73 μg cm^{-2}, respectively. For paddy rice in 2017, the mean Chl_a for T-1, T-2, and T-3 leaves were 54.13, 54.68 and 45.89 μg cm^{-2}, respectively. In 2018, the mean Chl_a values for the respective leaf layers of rice were 49.32, 52.32 and 48.53 μg cm^{-2}. The seasonal patterns of Chl_a across different leaf layers were similar for both winter wheat and paddy rice, but differed from those of N_a. The Chl_a in T-1 leaves initially increased, peaked at the flowering stage, remained high during the grain-filling, and then decreased rapidly at maturity. In contrast, the Chl_a in T-2 and T-3 leaves peaked at the jointing stage, maintained relatively high levels during the heading, flowering, grain-filling stages, and declined significantly by maturity.

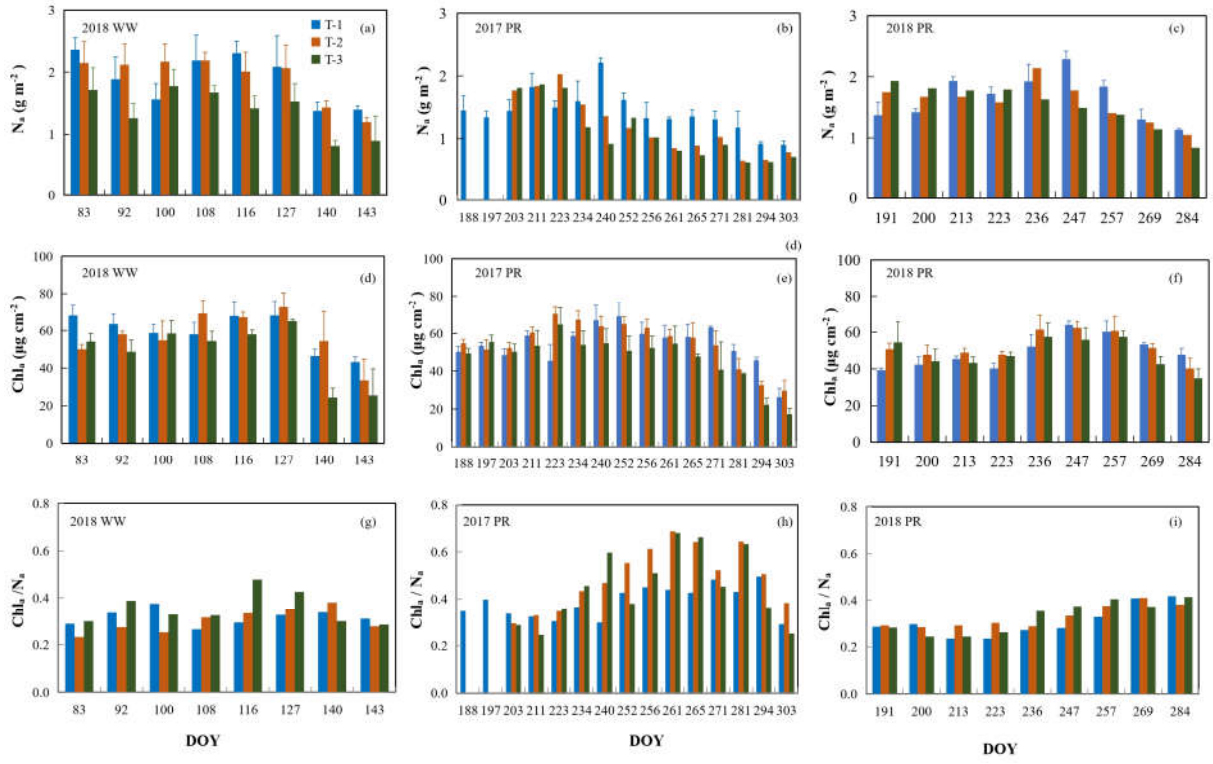

Figure 2. Temporal variations of N_a, Chl_a and Chl_a/N_a for winter wheat (WW) and paddy rice (PR). (a), (d) and (g) for winter wheat at SQOS in 2018; (b), (e) and (h) for paddy rice at JROS in 2017; (c), (f) and (i) for paddy rice at JROS in 2018. T-1 was the uppermost leaf, T-2 was the 2nd leaf from the top of the tiller, and T-3 was the 3rd leaf from the top of the tiller.

 doi:10.20944/preprints202604.0820.v1

The seasonal changes of the ratio of Chl_a to N_a (Chl_a/N_a) in leaves of each canopy layer of winter wheat and paddy rice are shown in Figure 2c, f, i. During the grain-filling to maturity stages, the Chl_a/N_a values in all leaf layers of both winter wheat and paddy rice exhibited a noticeable decline. When the data of winter wheat and rice were combined, the mean Chl_a/N_a value for T-1 leaves during the growing seasons was 0.35, while the mean values for T-2 and T-3 leaves were both approximately 0.39. This confirms that lower-canopy leaves, under low-light conditions, possess a relatively high chlorophyll content to capture light energy and enhance light use efficiency, which is a manifestation of the chlorophyll light compensation effect [38,39].

The relationships between Chl_a and N_a for leaves of winter wheat and paddy rice are shown in Figure 3. In general, there was a significant linear correlation between Chl_a and N_a in winter wheat and paddy rice, and the coefficient of determination R^2 was 0.374.

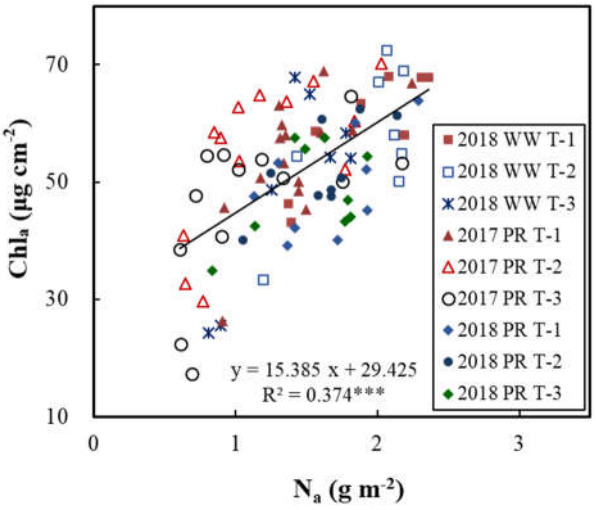

Figure 3. Relationships between Chl_a and N_a for leaves of winter wheat and paddy rice. *** represents the significance level of 0.001.

3.2. Seasonal Variations of Leaf V_{cmax25} and J_{max25} in Crop Canopies

The seasonal changes of V_{cmax25} and J_{max25} in leaves of different canopy layers of winter wheat and paddy rice are presented in Figure 4. For T-1 leaves of both species, V_{cmax25} and J_{max25} increased before flowering, peaked at this stage, and then declined rapidly. In contrast, T-2 and T-3 leaves exhibited earlier peaks: their V_{cmax25} and J_{max25} reached maxima at the jointing or heading stage, followed by gradual decreases. Across all growing seasons, a consistent vertical gradient was observed: V_{cmax25} and J_{max25} in T-1 > T-2 > T-3. Notably, both parameters were significantly higher in winter wheat than in paddy rice at all canopy layers.

During the 2018 growing season, V_{cmax25} in winter wheat leaves ranged from 19.03 to 118.23 μmol m^{-2} s^{-1}, with J_{max25} ranging from 31.79 to 252.88 μmol m^{-2} s^{-1}. Layer-specific means V_{cmax25} values revealed a stepwise decline: T-1 (91.07 μmol m^{-2} s^{-1}) > T-2 (83.11 μmol m^{-2} s^{-1}, ~91% of T-1) > T-3 (75.29 μmol m^{-2} s^{-1}, ~82% of T-1). J_{max25} followed a similar pattern, with layer means of 185.73 (T-1), 154.34 (T-2), and 135.98 μmol m^{-2} s^{-1} (T-3).

At JROS, V_{cmax25} and J_{max25} of 2017 and 2018 paddy rice leaves also showed significant seasonality. The average values of T-1, T-2 and T-3 V_{cmax25} in 2017 were 86.93, 71.70 and 56.21 μmol m^{-2} s^{-1}, respectively, and SD were 8.88, 7.19 and 8.84 μmol m^{-2} s^{-1}, respectively. The average J_{max25} values for T-1, T-2, and T-3 were 162.32, 139.65, and 103.2 μmol m^{-2} s^{-1}, respectively. In 2018, the average V_{cmax25} values of T-1, T-2 and T-3 were 82.26, 73.9 and 57.96 μmol m^{-2} s^{-1}, respectively, and the average J_{max25} values of T-1, T-2 and T-3 were 160.41, 141.15 and 119.16 μmol m^{-2} s^{-1}, respectively. A clear downward trend in both parameters was observed from the canopy top to the lower layers. In both years, the average V_{cmax25} of T-2 was approximately 85% of that in T-1, and T-3 V_{cmax25} was ~67% of T-1. Notably,

 doi:10.20944/preprints202604.0820.v1

these vertical reduction ratios were more pronounced in paddy rice than in winter wheat, indicating a steeper decline in photosynthetic capacity with depth in the rice canopy. The greater vertical heterogeneity in rice likely reflects its compact growth habit and the stronger light attenuation in dense rice canopies, which exacerbates resource limitations for lower-layer leaves.

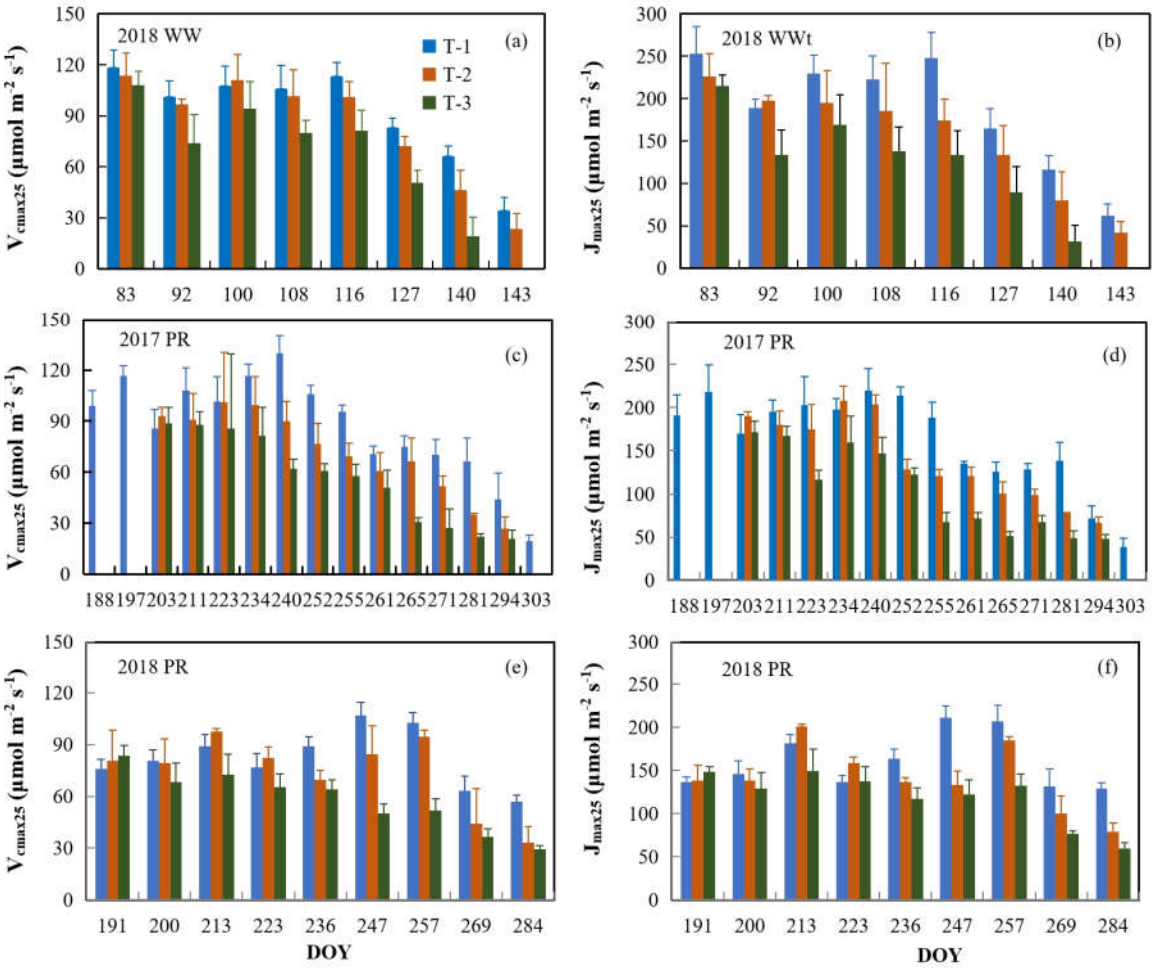

Figure 4. Seasonal variations of three leaf layers V_{cmax25} and J_{max25} of winter wheat and paddy rice. (a) and (b) for winter wheat at SQOS in 2018; (c) and (d) for paddy rice at JROS in 2017; (e) and (f) for paddy rice at JROS in 2018. T-1 is the uppermost leaf in the canopy. T-2 and T-3 are the 2nd and 3rd leaves from the top of a tiller.

There was a significant linear correlation between leaf V_{cmax25} and J_{max25} across different layers of wheat and paddy rice canopy (Figure 5). By integrating all the data of all paddy rice and winter wheat, the fitted linear equation of J_{max25} based on V_{cmax25} is:

$$J_{max25} = 1.919 \times V_{cmax25} + 1.162 \quad (1)$$

The R^2 of the fitted equation is 0.915, and and RMSE is 17.012 μmol m^{-2} s^{-1}, $p < 0.001$.

There was significant correlation between leaf V_{cmax25} in different layers of winter wheat and paddy rice canopy (Figure 6). The R^2 values were 0.790 for T-1 vs. T-2, 0.556 for T-1 vs. T-3, and 0.813 for T-2 vs. T-3 all reaching a significant level of 0.001. It is feasible to use the V_{cmax25} of the upper blade to estimate the V_{cmax25} of the lower leaves.

 doi:10.20944/preprints202604.0820.v1

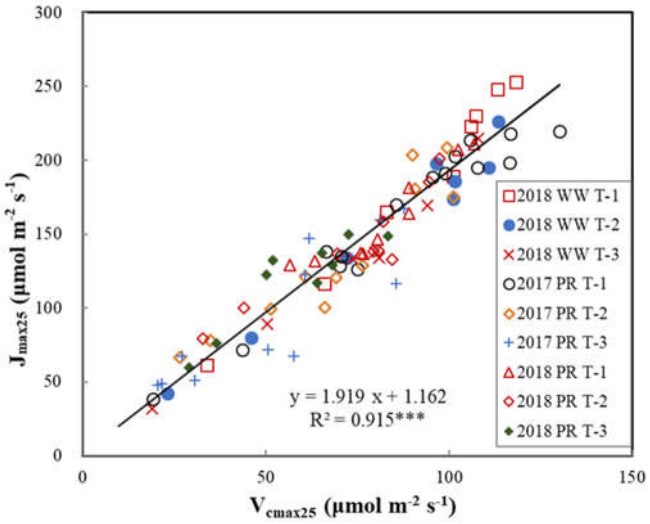

Figure 5. Relationships between V_{cmax25} and J_{max25} for all leaves of winter wheat (WW) and paddy rice (PR). T-1 is the uppermost leaf in the canopy. T-2 and T-3 are the 2nd and 3rd leaves from the top of a tiller. *** represents the significance level of 0.001.

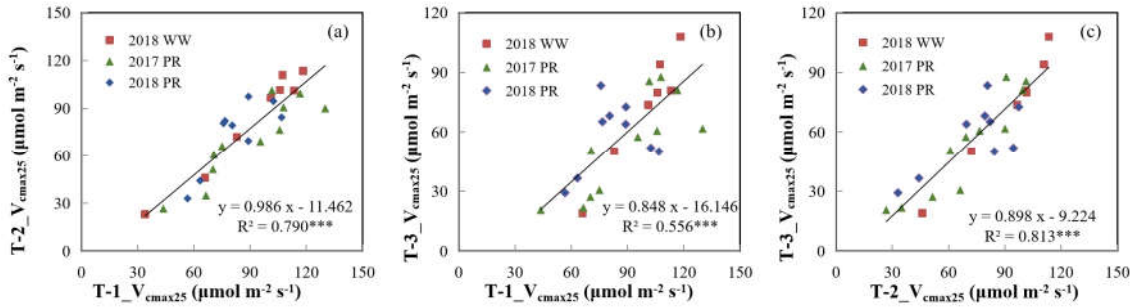

Figure 6. Relationships between V_{cmax25} at different layers of winter wheat (WW) and paddy rice (PR). *** represents the significance level of 0.001.

3.3. Relationships of V_{cmax25} with N_a and Chl$_a$

Figure 7 shows the linear correlation between V_{cmax25} and N_a in leaves of each inner layer of winter wheat and paddy rice canopy. For winter wheat and paddy rice, V_{cmax25} was significantly correlated with N_a ($p < 0.001$). Linear regression models ($V_{cmax25} = a \times N_a + b$) were established separately. N_a explained 51.3%, 59.1% and 66.9% of the seasonal variations of V_{cmax25} in T-1, T-2 and T-3 leaves of winter wheat and paddy rice, respectively, and the coefficient of determination R^2 increased with the downward position of leaves. The slopes of the linear regression equations for T-1, T-2 and T-3 are 46.05, 41.04 and 44.62, respectively, and the intercepts are 12.64, 12.23 and 0.34 μmol m^{-2} s^{-1}, respectively. We applied the dummy test to detect whether wheat and rice can be lumped together. The dummy variable was set to 1 for winter wheat and 0 for paddy rice to identify subsets of observations. Then, a multiple linear regression model was built with V_{cmax25} as the dependent variable and N_a as independent variables. The significance of individual coefficients of the multiple linear regression model was tested. It was found the differences in slopes ($p = 0.114$) and intercepts ($p = 0.351$) of regression models for winter wheat and rice were both failed to pass the significance test, suggesting the difference were insignificant.

By integrating the V_{cmax25} and N_a data of each layer of winter wheat in 2018 and paddy rice in 2017 and 2018 (Figure 7a), the following N_a-based V_{cmax25} estimation equation can be obtained:

$$V_{cmax25} = 45.916 \times N_a + 8.171 \quad (2)$$

 doi:10.20944/preprints202604.0820.v1

The result of comparing the estimated V_{cmax25} with the measured value is shown in Figure 8. The R^2 is 0.619, and RMSE is 15.751 μmol m^{-2} s^{-1}. In general, there is a good agreement between the estimated V_{cmax25} and the measured values. However, the low value of V_{cmax25} is overestimated and the high value is underestimated.

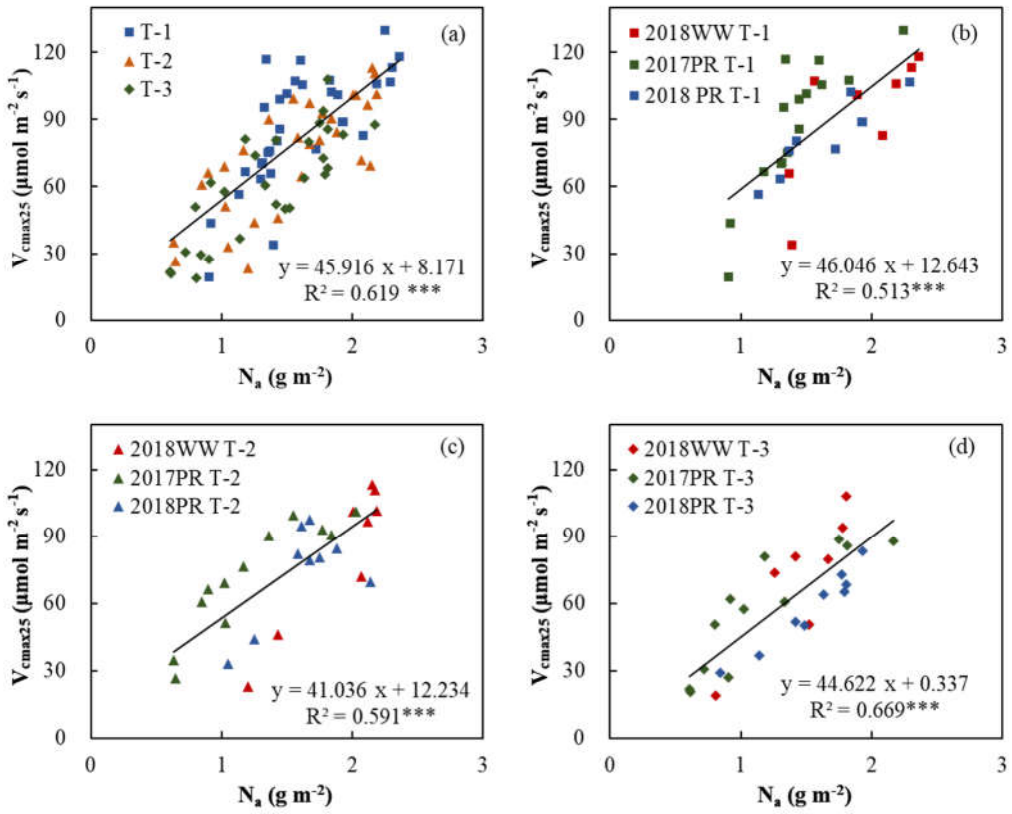

Figure 7. Changes of V_{cmax25} with N_a for winter wheat (WW) and paddy rice (PR). (a) for all samples of three layers. (b), (c) and (d) are for T-1, T-2 and T-3 samples, respectively. *** represents significance level of $p < 0.001$.

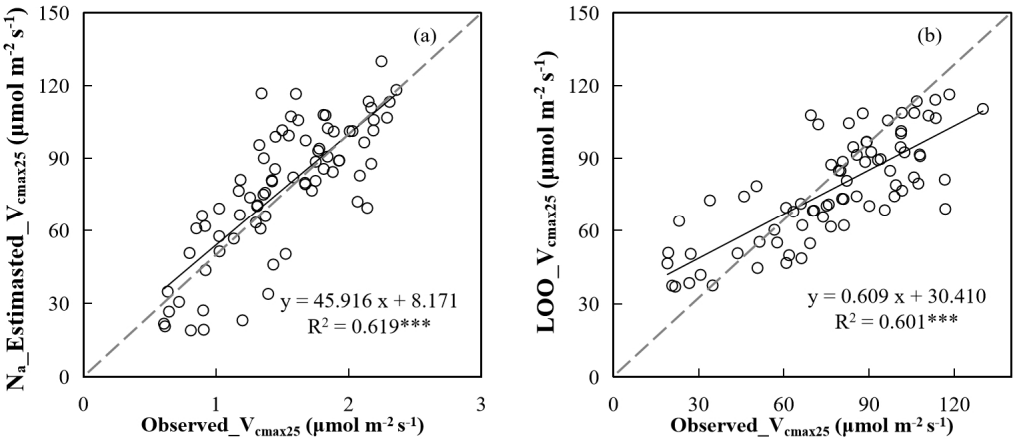

Figure 8. The comparison of estimated V_{cmax25} by N_a to observations (a) (RMSE = 15.751 μmol m^{-2} s^{-1}), and comparison of observed V_{cmax25} and V_{cmax25} estimated from leave one out (LOO-) cross validation (b) (RMSE = 17.245 μmol m^{-2} s^{-1}). *** represents significance indicator $p < 0.001$.

Figure 9 shows the variation characteristics of V_{cmax25} with Chl_a in different growth stages of winter wheat and paddy rice. There was a significant linear correlation between V_{cmax25} and Chl_a in all layers of winter wheat, and Chl_a could explain 41% (T-2) to 49% (T-1) of the seasonal variation of

 doi:10.20944/preprints202604.0820.v1

V_{cmax25}. The slope of the V_{cmax25} equation for T-1, T-2 and T-3 based on Chl_a is between 1.5-1.8, and the slope of T-1 is significantly greater than that of T-2 and T-3. The T-1 leaf has an intercept of -7.12 μmol m^{-2} s^{-1}, while the T-2 and T-3 have intercepts of -10.51 μmol m^{-2} s^{-1} and -17.82 μmol m^{-2} s^{-1} respectively. The V_{cmax25} of T-1 had the best correlation with Chl_a, while the V_{cmax25} of T-2 and T-3 had similar correlation with Chl_a. For all leaf layers of winter wheat and paddy rice, the V_{cmax25} estimation equation based on Chl_a is as follows (Figure 9a):

$$V_{cmax25} = 1.702 \times Chl_a - 15.846 \quad (3)$$

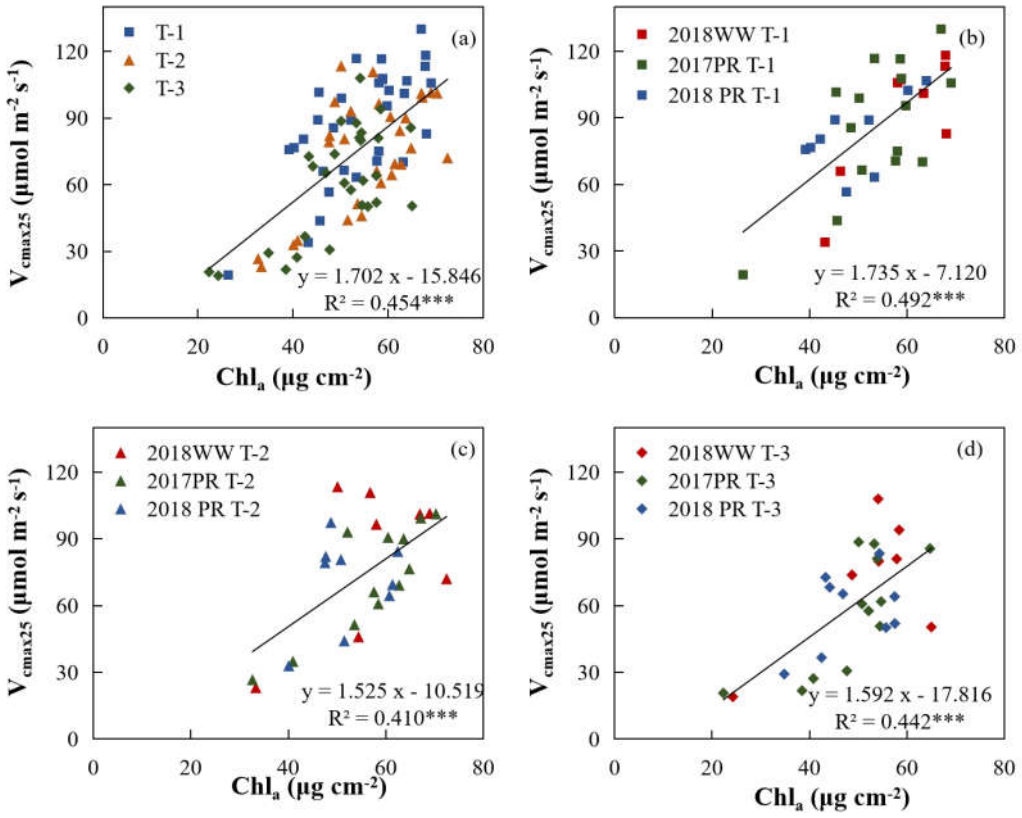

Figure 9. Changes of V_{cmax25} with Chl_a for winter wheat (WW) and paddy rice (PR). (a) for all samples of three layers. (b), (c) and (d) are for T-1, T-2 and T-3 samples, respectively. *** represents significance level of $p < 0.001$.

The RMSE of V_{cmax25} estimated by equation (3) compared with the observed data is 29.568 μmol m^{-2} s^{-1}, which is significantly higher than the RMSE of the N_a-based V_{cmax25} estimation model (15.751 μmol m^{-2} s^{-1}). It was found that the V_{cmax25} estimation model based on Chl_a was established before and after flowering, which could significantly improve the estimation accuracy of V_{cmax25} [21]. In this paper, for samples with T-1, T-2 and T-3 observation data at the same time, the necessity of establishing a Chl_a-based V_{cmax25} estimation model for leaves of different layers to distinguish between pre-flowering and post-flowering was analyzed. As shown in Figure 10a, for T-1 leaves, the estimation accuracy of V_{cmax25} could be significantly improved by distinguishing between pre-flowering and post-flowering stages, and the R^2 of pre-flowering and flowering stages was 0.731 and 0.756, which was significantly higher than that of the whole growth stage (0.492). For T-2 and T-3 leaves, modeling before and after flowering could not improve the estimation accuracy of V_{cmax25}. Dummy variable analysis showed that a unified Chl_a-based V_{cmax25} estimation model could be adopted for T-2 and T-3 blades (Figure 10).

The following three equations were used to estimate the V_{cmax25} of leaves of different layers:

T-1 pre-flowering: $V_{cmax25} = 1.372 \times Chl_a + 26.417$ $R^2 = 0.731$ (4)

T-1 post-flowering: $V_{cmax25}=1.903\times Chl_a-35.255$ $R^2 = 0.756$ (5)

 doi:10.20944/preprints202604.0820.v1

T-2 and T-3: $V_{cmax25}=1.660\times Chl_a-18.626$ $R^2 = 0.468$ (6)

A unified Chl_a based V_{cmax25} estimation model (Formula 3), without distinguishing between pre- and post- flowering and leaf position differences, would significantly overestimate the low value of V_{cmax25} and underestimate the high value of V_{cmax25} (Figure 11a). Differentiating T-1 from T-2 and T-3, and applying pre-flowering and post-flowering modeling strategies for T-1 (formulas 4, 5) can significantly improve the estimation accuracy of V_{cmax25} (Figure 11b). The R^2 and RMSE of the estimated V_{cmax25} compared with the observed data were 0.702 and 13.654 μmol m^{-2} s^{-1}.

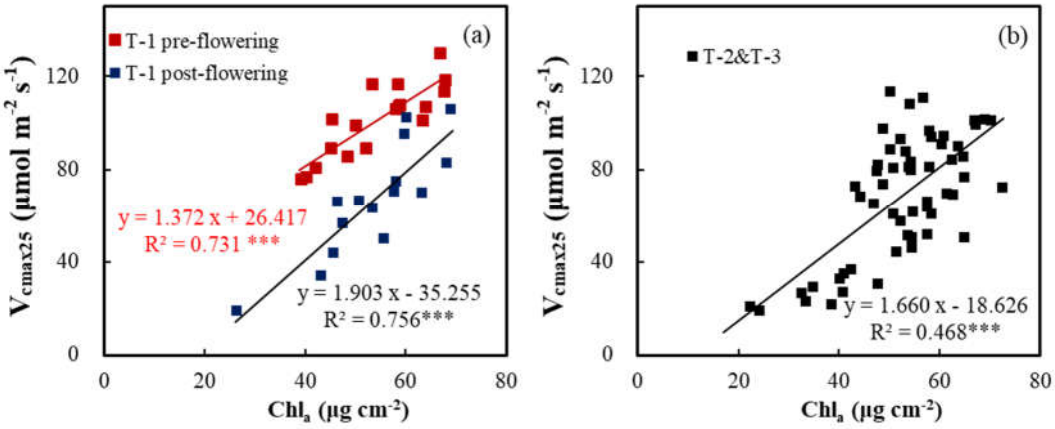

Figure 10. Relationships between V_{cmax25} and Chl_a for three layers of winter wheat and paddy rice. The red squares in (a) represent the T-1 leaves at pre-flowering stages, the blue represents the T-1 leaves at post-flowering stages, and the black square in (b) represents the T-2 and T-3 leaves.

Table 1. Correlations of V_{cmax25} with of N_a and Chl_a.*** indicate the significance levels of $p < 0.001$.

Group Description	Independent Variable	Slope	Intercept	R^2	Significance
T-1+T-2+T-3	N_a	45.916	8.171	0.619	***
T-1	N_a	46.046	12.643	0.513	***
T-2	N_a	41.036	12.234	0.591	***
T-3	N_a	44.622	0.337	0.669	***
T-1+T-2+T-3	Chl_a	1.702	-15.846	0.454	***
T-1	Chl_a	1.735	-7.120	0.492	***
T-2	Chl_a	1.525	-10.519	0.410	***
T-3	Chl_a	1.592	-17.816	0.442	***
T-1 pre-flowering	Chl_a	1.372	26.417	0.731	***
T-1 post-flowering	Chl_a	1.903	-35.255	0.756	***
T-2 + T-3	Chl_a	1.660	-18.626	0.468	***

 doi:10.20944/preprints202604.0820.v1

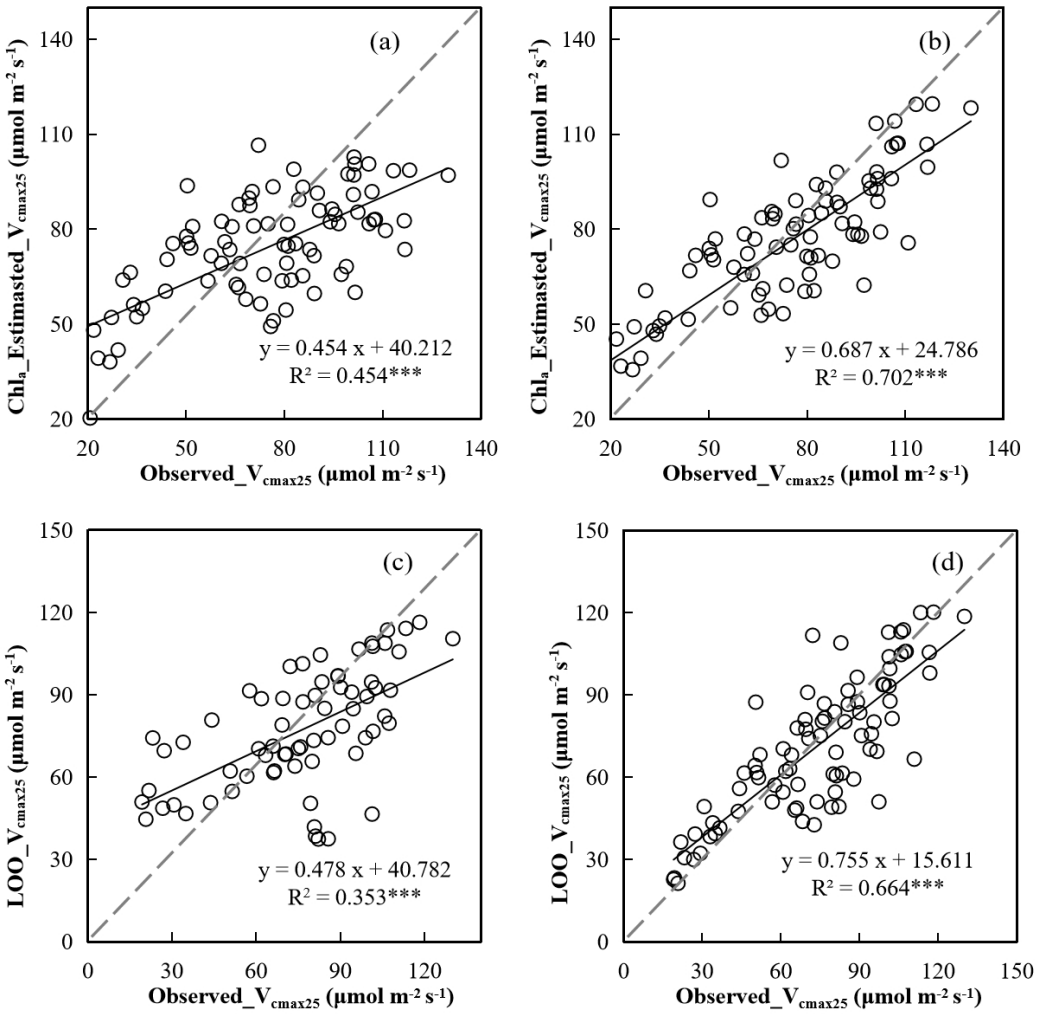

Figure 11. The comparison of V_{cmax25} estimated from Chl_a with observations. (a) V_{cmax25} estimated using the same model for different layers and growing stages (Equation 3), and (c) V_{cmax25} estimated from leave one out (LOO-) cross validation accordingly; (b) V_{cmax25} estimated using the different models for different layers and for T-1 at different stages (Equations 4, 5 and 6), and (d) V_{cmax25} estimated from leave one out (LOO-) cross validation accordingly. *** represents significance level of 0.001.

4. Discussion

4.1. Difference in Vertical Patterns of Photosynthetic and Biochemical Parameters

Many studies have analyzed the vertical differences of photosynthetic and biochemical parameters of leaves at different positions within the canopy of crops [34,38–42]. However, most studies focus on a certain growth period of crops, and it is difficult to fully characterize the vertical changes of photosynthetic and biochemical parameters of leaves at different growth stages and positions of crops. In order to make up for this shortcoming, the biochemical and photosynthetic parameters of different growth stages and different leaf positions were observed in winter wheat and paddy rice fields, and their seasonal differences were analyzed.

Chl_a in the upper canopy (T-1) peaked at flowering and remained elevated until milk-ripening, whereas middle layers (T-2 and T-3) retained high Chl_a levels from jointing to maturity before sharp declines at senescence (Figure 2). This pattern aligns with the "light compensation effect," where shaded leaves prioritize Chl_a retention to enhance light capture efficiency under limited light conditions [40,41]. In contrast, N_a demonstrated a more uniform vertical decline, with T-1 values

 doi:10.20944/preprints202604.0820.v1

decreasing rapidly post-flowering and T-2/T-3 following at jointing-head stages. The delayed Chl_a decline compared to N_a in middle layers suggests a physiological trade-off: maintaining Chl_a content for light absorption despite reduced nitrogen availability, likely due to its role in light-harvesting complexes rather than direct nitrogen storage [42].

The vertical gradients of V_{cmax25} and J_{max25}, key indicators of photosynthetic capacity, were tightly linked to leaf age and canopy position. Both parameters exhibited a pronounced stepwise decline from T-1 to T-3 across growth stages, with T-1 values peaking at flowering and decreasing sharply thereafter (Figure 4). This trend mirrors findings in forests, where photosynthetic capacity parameters showed strict proportionality to light availability and leaf nitrogen content [43–45]. The accelerated decline of V_{cmax25}/J_{max25} in lower layers (T-3) compared to Chl_a can be attributed to Rubisco enzyme degradation during leaf senescence, which directly impacts carboxylation efficiency but leaves pigments (Chl_a) relatively stable until advanced senescence [46].

4.2. The Ability of Chl_a and N_a to Characterize V_{cmax25} of Leaves at Different Positions in the Canopy

Our results demonstrate that both N_a and Chl_a serve as reliable proxies for estimating V_{cmax25}, but their predictive power varies significantly across canopy layers. The strong correlations observed between N_a/Chl_a and V_{cmax25} (Figures 7, 9) align with the physiological premise that Rubisco content—the primary determinant of carboxylation capacity—scales with both nitrogen allocation and chlorophyll abundance[1,21]. The integrated data analysis of Luo et al. [28] showed that there was no significant difference in the relationship between Chl_a content and Rubisco content among C3 crops. The observational data in our study proved that for T-1, T-2 and T-3 leaves, the same V_{cmax25} estimation equation based on N_a and Chl_a could be used for both winter wheat and paddy rice. However, the strength of these relationships exhibited notable vertical stratification.

N_a demonstrated superior predictive capability compared to Chl_a, particularly in middle layers, where Rubisco degradation outpaced chlorophyll breakdown during senescence [47,48]. This divergence stems from fundamental differences in their physiological roles: Rubisco degradation is directly linked to leaf aging and photooxidative stress, whereas Chl_a retention in shaded layers represents an adaptive strategy for maximizing light capture under limited radiation [23]. Our modeling approach revealed that while a unified N_a-based model provided reasonable accuracy across all layers ($R^2 = 0.619$, RMSE = 15.751 μmol m^{-2} s^{-1}), layer-specific differentiation substantially improved Chl_a-based estimations. For T-1 leaves, separate pre- and post-flowering models (Equations 4-5) increased R^2 from 0.492 to 0.731-0.756, capturing phenological shifts in nitrogen allocation priorities. In contrast, T-2 and T-3 leaves maintained consistent Chl_a-V_{cmax25} relationships throughout development (Equation 6), reflecting their more stable light environment and gradual senescence pattern.

4.3. Implications and Uncertainties in Remote Sensing of Canopy Photosynthetic Capacity

The vertical heterogeneity in photosynthetic parameters revealed by our study has profound implications for remote sensing-based monitoring of crop productivity. Current vegetation indices, such as those derived from multispectral sensors, predominantly capture signals from the upper canopy, potentially overlooking the significant contributions of middle and lower layers to overall carbon assimilation [49]. Our finding that T-2 and T-3 leaves maintain substantial photosynthetic activity throughout much of the growing season underscores the need for vertical stratification in canopy photosynthesis models. The demonstrated relationships between N_a/Chl_a and V_{cmax25} offer promising pathways for improving remote sensing retrievals. Hyperspectral indices sensitive to chlorophyll and nitrogen content could be calibrated with layer-specific coefficients to account for vertical gradients [23]. Multi-angle observation techniques show particular promise, as they can penetrate deeper into the canopy and provide information on the vertical distribution of biochemical traits [50,51]. By integrating our measured relationships between photosynthetic parameters and pigment content (Figures 7-11), future studies could develop mechanistic links between canopy reflectance spectra and vertically-resolved photosynthetic capacity.

 doi:10.20944/preprints202604.0820.v1

Several uncertainties must be acknowledged in translating our findings to regional applications. The leaf-level measurements presented here, while detailed, represent discrete points in time and space. Our use of different leaf samples for photosynthetic versus biochemical measurements, though necessary for logistical reasons, may introduce uncertainty in the observed correlations. Furthermore, the single-year dataset for winter wheat limits our ability to capture interannual variability in parameter relationships. Additionally, the biological replication at each sampling event was limited to three plants per crop per site—a common constraint in field gas exchange studies due to the destructive and time-intensive nature of A_n-C_i curve measurements. While our total dataset comprises hundreds of leaf-level observations across multiple phenological stages and two years for rice, this per-event replication level warrants caution in overgeneralizing the derived models. The focus on functional leaves (T-1 to T-3) provides valuable insights for yield formation periods but neglects the contributions of lower canopy strata. In dense canopies, these lower layers may significantly influence overall canopy conductance and carbon cycling. Additionally, the interaction between leaf age and position warrants further investigation, as these factors collectively determine photosynthetic efficiency but are difficult to disentangle in field observations.

5. Conclusions

Our study systematically analyzed the vertical distribution of photosynthetic and biochemical parameters (V_{cmax25}, J_{max25}, leaf nitrogen content (N_a), and chlorophyll (Chl_a)) across canopy layers in winter wheat and paddy rice, revealing dynamic adaptive mechanisms of canopy photosynthesis. The main conclusions are as follows:

(1) Significant vertical heterogeneity in photosynthetic parameters, with V_{cmax25} and J_{max25} exhibiting a consistent stepwise decline from T-1 to T-3, driven by Rubisco enzyme activity and leaf senescence

(2) T-1 V_{cmax25} peaked at flowering, while T-2/T-3 peaked earlier (heading/jointing stages), aligning with N_a dynamics while lagging Chl_a decline - a pattern suggestive of a strategy to retain Chl_a for weak-light capture.

(3) A unified N_a-based V_{cmax25} model ($R^2 = 0.619$) demonstrated promising general applicability, with Chl_a-based models requiring separation of T-1 from T-2/T-3 due to Rubisco degradation-light compensation trade-offs. N_a outperformed Chl_a in characterizing vertical V_{cmax25} variation, supporting the potential value of layered parameterization in canopy photosynthesis models to enhance simulation precision.

Our findings demonstrate that acknowledging vertical heterogeneity in photosynthetic parameters is essential for accurate monitoring and modeling of crop productivity. The integration of layer-specific biochemical-photosynthetic relationships with advanced remote sensing techniques holds great promise for advancing precision agriculture and improving yield predictions in a changing climate. Future multi-site, multi-year studies with larger replication are needed to validate and refine the models proposed here.

Author Contributions: Conceptualization, J.L., W.J. and B.T.; methodology, J.L. and Y.Z.; formal analysis, J.L., X.L., Y.Z., W.J. and K.C.; investigation, J.L., X.L., and T.Z.; resources, B.T. and W.J.; data curation, J.L., S.S.; writing—original draft preparation, J.L., Y.Z., W.J., B.T., S.S.; writing—review and editing, J.L., Y.Z., X.L., T.Z., K.C., S.S., B.T. W.J.; visualization, J.L., Y.Z.; supervision, B.T. and W.J.; project administration, W.J. and B.T. contributed equally to this work. Every author made intellectual contributions throughout the research design and manuscript preparation phases, leveraging their individual areas of expertise. All authors have read and agreed to the published version of the manuscript.

Funding: This research was funded by the Zhejiang Provincial Soft Science Research Program (Grants No. 2025C35016) and the Zhejiang Provincial Program for Environmental Scientific Research and Demonstration of Achievements (Grants No. 2024HT0075).

Institutional Review Board Statement: Not applicable.

 doi:10.20944/preprints202604.0820.v1

Data Availability Statement: The data supporting this study's findings are available from the corresponding author upon reasonable request.

Acknowledgments: We are greatly grateful to the staff of the National Field Scientific Observation and Research Station of Agro-ecosystem in Shangqiu, Henan Province for their valuable assistance during our experiment.

Conflicts of Interest: The authors declare no conflicts of interest.

References

1. Kang, M.; Zhang, L.; Qin, T.; An, J.; Wang, C.; Wang, S.; Ali, I.; Liu, B.; Liu, L.; Tang, L.; et al. Bridging Chlorophyll Content and Vertical Nitrogen Distribution for Accurate Canopy Photosynthesis Simulation. *Computers and Electronics in Agriculture* **2025**, *239*, 110885, doi:10.1016/j.compag.2025.110885.
2. Kaneko, T.; Nomura, K.; Yasutake, D.; Iwao, T.; Okayasu, T.; Ozaki, Y.; Mori, M.; Hirota, T.; Kitano, M. A Canopy Photosynthesis Model Based on a Highly Generalizable Artificial Neural Network Incorporated with a Mechanistic Understanding of Single-Leaf Photosynthesis. *Agricultural and Forest Meteorology* **2022**, *323*, 109036, doi:10.1016/j.agrformet.2022.109036.
3. Kull, O.; Jarvis, P.G. The Role of Nitrogen in a Simple Scheme to Scale up Photosynthesis from Leaf to Canopy. *Plant, Cell & Environment* **1995**, *18*, 1174–1182, doi:10.1111/j.1365-3040.1995.tb00627.x.
4. Kull, O. Acclimation of Photosynthesis in Canopies: Models and Limitations. *Oecologia* **2002**, *133*, 267–279, doi:10.1007/s00442-002-1042-1.
5. Kenzo, T.; Ichie, T.; Watanabe, Y.; Yoneda, R.; Ninomiya, I.; Koike, T. Changes in Photosynthesis and Leaf Characteristics with Tree Height in Five Dipterocarp Species in a Tropical Rain Forest. *Tree Physiol* **2006**, *26*, 865–873, doi:10.1093/treephys/26.7.865.
6. Legner, N.; Fleck, S.; Leuschner, C. Within-Canopy Variation in Photosynthetic Capacity, SLA and Foliar N in Temperate Broad-Leaved Trees with Contrasting Shade Tolerance. *Trees* **2014**, *28*, 263–280, doi:10.1007/s00468-013-0947-0.
7. D'Odorico, P.; Emmel, C.; Revill, A.; Liebisch, F.; Eugster, W.; Buchmann, N. Vertical Patterns of Photosynthesis and Related Leaf Traits in Two Contrasting Agricultural Crops. *Functional Plant Biology* **2019**, *46*, 213–227, doi:10.1071/FP18061.
8. Niinemets, Ü. Variation in Leaf Photosynthetic Capacity within Plant Canopies: Optimization, Structural, and Physiological Constraints and Inefficiencies. *Photosynthesis research* **2023**, *158*, doi:10.1007/s11120-023-01043-9.
9. Ma, X.R.; Song, X.M.; Zhang, E.Z.; Du, J.B.; Sun, X. Role of Nitrogen Utilization in Facilitating Photosynthetic Compensation of Soybean under Vertically Heterogeneous Light. *Photosynt.* **2025**, *63*, 291–295, doi:10.32615/ps.2025.026.
10. Archontoulis, S.V.; Vos, J.; Yin, X.; Bastiaans, L.; Danalatos, N.G.; Struik, P.C. Temporal Dynamics of Light and Nitrogen Vertical Distributions in Canopies of Sunflower, Kenaf and Cynara. *Field Crops Research* **2011**, *122*, 186–198, doi:10.1016/j.fcr.2011.03.008.
11. Lemaire, G.; Onillon, B.; Gosse, G.; Chartier, M.; Allirand, J.M. Nitrogen Distribution within a Lucerne Canopy during Regrowth: Relation with Light Distribution. *Annals of Botany* **1991**, *68*, 483–488.
12. Sultana, F.; Dev, W.; Xin, M.; Han, Y.; Feng, L.; Lei, Y.; Yang, B.; Wang, G.; Li, X.; Wang, Z.; et al. Competition for Light Interception in Different Plant Canopy Characteristics of Diverse Cotton Cultivars. *Genes (Basel)* **2023**, *14*, 364, doi:10.3390/genes14020364.
13. Meir, P.; Kruijt, B.; Broadmeadow, M.; Kull, O.; Carswell, F.; Nobre, A. Acclimation of Photosynthetic Capacity to Irradiance in Tree Canopies in Relation to Leaf Nitrogen Concentration and Leaf Mass per Unit Area. *Plant, Cell and Environment* **2002**, *25*, 343–357, doi:10.1046/j.0016-8025.2001.00811.x.
14. Farquhar, G.D.; von Caemmerer, S.; Berry, J.A. A Biochemical Model of Photosynthetic CO 2 Assimilation in Leaves of C 3 Species. *Planta* **1980**, *149*, 78–90.
15. Wullschleger, S.D. Biochemical Limitations to Carbon Assimilation in C 3 Plants—a Retrospective Analysis of the a/C i Curves from 109 Species. *Journal of Experimental Botany* **1993**, *44*, 907–920.
16. Walker, A.P.; Beckerman, A.P.; Gu, L.; Kattge, J.; Cernusak, L.A.; Domingues, T.F.; Scales, J.C.; Wohlfahrt, G.; Wullschleger, S.D.; Woodward, F.I. The Relationship of Leaf Photosynthetic Traits - V Cmax and J Max

 doi:10.20944/preprints202604.0820.v1

- to Leaf Nitrogen, Leaf Phosphorus, and Specific Leaf Area: A Meta-Analysis and Modeling Study. *Ecol Evol* **2014**, *4*, 3218–3235, doi:10.1002/ece3.1173.

17. Wang, X.; Shi, J. Leaf Chlorophyll Content Is the Crucial Factor for the Temporal and Spatial Variation of Global Plants Leaf Maximum Carboxylation Rate. *Science of The Total Environment* **2024**, *927*, 172280, doi:10.1016/j.scitotenv.2024.172280.
18. Ali, A.A.; Xu, C.; Rogers, A.; McDowell, N.G.; Medlyn, B.E.; Fisher, R.A.; Wullschleger, S.D.; Reich, P.B.; Vrugt, J.A.; Bauerle, W.L.; et al. Global-Scale Environmental Control of Plant Photosynthetic Capacity. *Ecological Applications* **2015**, *25*, 2349–2365, doi:10.1890/14-2111.1.
19. Wu, J.; Rogers, A.; Albert, L.P.; Ely, K.; Prohaska, N.; Wolfe, B.T.; Oliveira Jr, R.C.; Saleska, S.R.; Serbin, S.P. Leaf Reflectance Spectroscopy Captures Variation in Carboxylation Capacity across Species, Canopy Environment and Leaf Age in Lowland Moist Tropical Forests. *New Phytologist* **2019**, *224*, 663–674, doi:10.1111/nph.16029.
20. Rogers, A.; Serbin, S.P.; Ely, K.S.; Sloan, V.L.; Wullschleger, S.D. Terrestrial Biosphere Models Underestimate Photosynthetic Capacity and CO2 Assimilation in the Arctic. *New Phytol* **2017**, *216*, 1090–1103, doi:10.1111/nph.14740.
21. Li, J.; Lu, X.; Ju, W.; Li, J.; Zhu, S.; Zhou, Y. Seasonal Changes of Leaf Chlorophyll Content as a Proxy of Photosynthetic Capacity in Winter Wheat and Paddy Rice. *Ecological Indicators* **2022**, *140*, 109018, doi:10.1016/j.ecolind.2022.109018.
22. Qian, X.; Zhang, Y.; Liu, L. Growth-Stage-Dependent Relationship between Photosynthetic Capacity and Leaf Biochemical Traits in Cotton. *Industrial Crops and Products* **2025**, *235*, 121650, doi:10.1016/j.indcrop.2025.121650.
23. Chen, J.M.; Wang, R.; Liu, Y.; He, L.; Croft, H.; Luo, X.; Wang, H.; Smith, N.G.; Keenan, T.F.; Prentice, I.C.; et al. Global Datasets of Leaf Photosynthetic Capacity for Ecological and Earth System Research.
24. Croft, H.; Chen, J.M.; Luo, X.; Bartlett, P.; Chen, B.; Staebler, R.M. Leaf Chlorophyll Content as a Proxy for Leaf Photosynthetic Capacity. *Glob Chang Biol* **2017**, *23*, 3513–3524, doi:10.1111/gcb.13599.
25. Niinemets, Ü.; Keenan, T.F.; Hallik, L. A Worldwide Analysis of Within-Canopy Variations in Leaf Structural, Chemical and Physiological Traits across Plant Functional Types. *New Phytologist* **2015**, *205*, 973–993, doi:10.1111/nph.13096.
26. Niinemets, U. Photosynthesis and Resource Distribution through Plant Canopies. *Plant Cell Environ* **2007**, *30*, 1052–1071, doi:10.1111/j.1365-3040.2007.01683.x.
27. Chen, J.M.; Liu, J.; Cihlar, J.; Goulden, M.L. Daily Canopy Photosynthesis Model through Temporal and Spatial Scaling for Remote Sensing Applications. *Ecological Modelling* **1999**, *124*, 99–119, doi:10.1016/S0304-3800(99)00156-8.
28. Luo, X.; Croft, H.; Chen, J.M.; He, L.; Keenan, T.F. Improved Estimates of Global Terrestrial Photosynthesis Using Information on Leaf Chlorophyll Content. *Global Change Biology* **2019**, *25*, 2499–2514, doi:10.1111/gcb.14624.
29. Ye, M.; Wu, M.; Zhang, Y.; Wang, Z.; Zhang, H.; Zhang, Z. Physiological Factors Limiting Leaf Net Photosynthetic Rate in C3 Crops like Rice and Approaches for Improving It. *Agronomy* **2022**, *12*, 1830, doi:10.3390/agronomy12081830.
30. Albert, L.P.; Wu, J.; Prohaska, N.; de Camargo, P.B.; Huxman, T.E.; Tribuzy, E.S.; Ivanov, V.Y.; Oliveira, R.S.; Garcia, S.; Smith, M.N.; et al. Age-Dependent Leaf Physiology and Consequences for Crown-Scale Carbon Uptake during the Dry Season in an Amazon Evergreen Forest. *New Phytologist* **2018**, *219*, 870–884, doi:10.1111/nph.15056.
31. Dai, S.; Ju, W.; Zhang, Y.; He, Q.; Song, L.; Li, J. Variations and Drivers of Methane Fluxes from a Rice-Wheat Rotation Agroecosystem in Eastern China at Seasonal and Diurnal Scales. *Science of The Total Environment* **2019**, *690*, 973–990, doi:10.1016/j.scitotenv.2019.07.012.
32. Li, J.; Zhang, Y.; Gu, L.; Li, Z.; Li, J.; Zhang, Q.; Zhang, Z.; Song, L. Seasonal Variations in the Relationship between Sun-Induced Chlorophyll Fluorescence and Photosynthetic Capacity from the Leaf to Canopy Level in a Rice Crop. *J Exp Bot* **2020**, *71*, 7179–7197, doi:10.1093/jxb/eraa408.

 doi:10.20944/preprints202604.0820.v1

33. Lu, X.; Ju, W.; Li, J.; Croft, H.; Chen, J.M.; Luo, Y.; Yu, H.; Hu, H. Maximum Carboxylation Rate Estimation with Chlorophyll Content as a Proxy of Rubisco Content. *Journal of Geophysical Research: Biogeosciences* **2020**, *125*, e2020JG005748, doi:10.1029/2020JG005748.
34. Li, T.; Angeles, O.; Marcaida, M.; Manalo, E.; Manalili, M.P.; Radanielson, A.; Mohanty, S. From ORYZA2000 to ORYZA (v3): An Improved Simulation Model for Rice in Drought and Nitrogen-Deficient Environments. *Agricultural and Forest Meteorology* **2017**, *237–238*, 246–256, doi:10.1016/j.agrformet.2017.02.025.
35. Duursma, R.A. Plantecophys - an R Package for Analysing and Modelling Leaf Gas Exchange Data. *PLoS ONE* **2015**, *10*, e0143346, doi:10.1371/journal.pone.0143346.
36. Long, S.P.; Bernacchi, C.J. Gas Exchange Measurements, What Can They Tell Us about the Underlying Limitations to Photosynthesis? Procedures and Sources of Error. *Journal of Experimental Botany* **2003**, *54*, 2393–2401.
37. Gujarati, D. Use of Dummy Variables in Testing for Equality between Sets of Coefficients in Linear Regressions: A Generalization. *The American Statistician* **1970**, *24*, 18–22, doi:10.2307/2682446.
38. Zhang, C.; Yi, Y.; Zhang, S.; Li, P. Quantitative Analysis of Vertical and Temporal Variations in the Chlorophyll Content of Winter Wheat Leaves via Proximal Multispectral Remote Sensing and Deep Transfer Learning. *Agriculture* **2024**, *14*, 1685, doi:10.3390/agriculture14101685.
39. Lambers, H.; Chapin III, F.S.; Pons, T. *Plant Physiological Ecology: Second Edition*; 2008; p. 604; ISBN 978-0-387-78340-6.
40. Wang, Z.; Wang, J.; Zhao, C.; Zhao, M.; Huang, W.; Wang, C. Vertical Distribution of Nitrogen in Different Layers of Leaf and Stem and Their Relationship with Grain Quality of Winter Wheat. *Journal of Plant Nutrition* **2005**, *28*, 73–91, doi:10.1081/PLN-200042175.
41. Šimpraga, M.; Verbeeck, H.; Bloemen, J.; Vanhaecke, L.; Demarcke, M.; Joó, E.; Pokorska, O.; Amelynck, C.; Schoon, N.; Dewulf, J.; et al. Vertical Canopy Gradient in Photosynthesis and Monoterpenoid Emissions: An Insight into the Chemistry and Physiology Behind. *Atmospheric Environment* **2013**, *80*, 85–95, doi:10.1016/j.atmosenv.2013.07.047.
42. Yu, W.; Ji, R.; Jia, Q.; Feng, R.; Wu, J.; Zhang, Y. Vertical Distribution Characteristics of Photosynthetic Parameters for *Phragmites Australis* in Liaohe River Delta Wetland, China. *Journal of Freshwater Ecology* **2017**, *32*, 557–573, doi:10.1080/02705060.2017.1358677.
43. Song, G.; Wang, Q.; Jin, J. Exploring the Instability of the Relationship between Maximum Potential Electron Transport Rate and Maximum Carboxylation Rate in Cool-Temperate Deciduous Forests. *Agricultural and Forest Meteorology* **2021**, *308–309*, 108614, doi:10.1016/j.agrformet.2021.108614.
44. Zhuang, J.; Zhou, L.; Wang, Y.; Chi, Y. Nitrogen Allocation Regulates the Relationship between Maximum Carboxylation Rate and Chlorophyll Content along the Vertical Gradient of Subtropical Forest Canopy. *Agricultural and Forest Meteorology* **2021**, *307*, 108512, doi:10.1016/j.agrformet.2021.108512.
45. Wu, J.; Serbin, S.P.; Xu, X.; Albert, L.P.; Chen, M.; Meng, R.; Saleska, S.R.; Rogers, A. The Phenology of Leaf Quality and Its Within-Canopy Variation Is Essential for Accurate Modeling of Photosynthesis in Tropical Evergreen Forests. *Global Change Biology* **2017**, *23*, 4814–4827, doi:10.1111/gcb.13725.
46. Li, H.W.; Zhang, J.; Zheng, Q.; Li, B.; Li, Z.S. Comparative Study of Photosynthetic Capacity in Lower Leaves in the Canopy of Dwarf and Semidwarf Wheat. *Photosynthetica* **2022**, *60*, 445–456, doi:10.32615/ps.2022.037.
47. Davidson, K.J.; Lamour, J.; McPherran, A.; Rogers, A.; Serbin, S.P. Seasonal Trends in Leaf-Level Photosynthetic Capacity and Water Use Efficiency in a North American Eastern Deciduous Forest and Their Impact on Canopy-Scale Gas Exchange. *New Phytol* **2023**, *240*, 138–156, doi:10.1111/nph.19137.
48. Ding, H.; Wang, Z.; Zhang, Y.; Li, J.; Jia, L.; Chen, Q.; Ding, Y.; Wang, S. A Mechanistic Model for Estimating Rice Photosynthetic Capacity and Stomatal Conductance from Sun-Induced Chlorophyll Fluorescence. *Plant Phenomics* **2023**, *5*, doi:10.34133/plantphenomics.0047.
49. Yan, Z.; Guo, Z.; Serbin, S.P.; Song, G.; Zhao, Y.; Chen, Y.; Wu, S.; Wang, J.; Wang, X.; Li, J.; et al. Spectroscopy Outperforms Leaf Trait Relationships for Predicting Photosynthetic Capacity across Different Forest Types. *New Phytologist* **2021**, *232*, 134–147, doi:10.1111/nph.17579.

 doi:10.20944/preprints202604.0820.v1

50. Beck, P.S.A.; Atzberger, C.G.; Høgda, K.A.; Johansen, B.; Skidmore, A.K. Improved Monitoring of Vegetation Dynamics at Very High Latitudes: A New Method Using MODIS NDVI. *REMOTE SENS ENVIRON* **2006**, *100*, 321–334, doi:10.1016/j.rse.2005.10.021.
51. Bin Wu; Fan, L.; Xu, B.; Yang, J.; Zhao, R.; Wang, Q.; Ai, X.; Zhao, H.; Yang, Z. UAV-Based LiDAR and Multispectral Sensors Fusion for Cotton Yield Estimation: Plant Height and Leaf Chlorophyll Content as a Bridge Linking Remote Sensing Data to Yield. *Industrial Crops and Products* **2025**, *230*, 121110, doi:10.1016/j.indcrop.2025.121110.